J. Phys. France **50** (1989) 3477-3487 15 DÉCEMBRE **1989,** PAGE 3477

Classification
Physics Abstracts
64.70K — 77.80 — 78.30

Phonon spectra of $NH_4H_2PO_4$ in the para- and antiferroelectric phases obtained by infrared reflectivity

Patrick Simon

C.R.P.H.T. - C.N.R.S., 45071 Orléans Cedex 2, France

(*Reçu le 13 juillet 1989, accepté le 11 septembre 1989*)

Résumé. — On présente les spectres de réflexion infrarouge de $NH_4H_2PO_4$ en lumière polarisée, sur une large gamme spectrale (20-1 500 cm^{-1}), dans les phases para- et antiferroélectriques. Les mesures ont pu être effectuées dans la phase basse température bien que les cristaux se brisent systématiquement à la transition de phase. Les spectres de phonons sont obtenus en simulant les spectres expérimentaux à l'aide de la forme factorisée de la fonction diélectrique. La conséquence la plus nette de la transition de phase sur les spectres de phonons est la disparition juste au-dessous de T_N d'un mode de basse fréquence, très amorti, dans les deux polarisations. Ce mode provient du mouvement intersites des protons, et est couplé avec l'instabilité antiferroélectrique en bord de zone de Brillouin. Les autres modes de réseau ne sont que peu affectés par la transition de phase, en particulier les modes internes des groupements NH_4. L'ensemble des résultats est discuté et comparé avec un travail récent sur les composés ferroélectriques du type KH_2PO_4, ce qui permet d'attribuer les modes de réseau et de confirmer le rôle d'un mode interne au tétraèdre PO_4 dans le mécanisme d'apparition de la ferroélectricité dans ces composés.

Abstract. — The polarized infrared reflectivity spectra of $NH_4H_2PO_4$ are reported for a wide spectral range (20-1 500 cm^{-1}) in the para- and antiferroelectric phases. Measurements were performed despite the shattered character of the sample in the low-temperature phase. The phonon spectra are obtained by fitting the factorized form of the dielectric function to the experimental spectra. The most marked effect on the experimental spectra at the phase transition is the disappearance of a highly-damped low-frequency mode upon cooling below T_N, in both polarizations. This mode originates from intersite proton motions, and is coupled with the Brillouin zone-corner antiferroelectric instability. The other modes are only slightly affected by the phase transition, especially the NH_4 internal modes. The results are discussed in the light of a previous work on ferroelectric KH_2PO_4-type compounds, which enables to assign the lattice modes, and to confirm the role of an internal PO_4 mode in the mechanism of ferroelectricity in these compounds.

1. Introduction.

Hydrogen-bonded compounds of the KH_2PO_4-type (KDP) undergo a paraelectric (PE)-ferroelectric (FE) phase transition at low temperature [1, 2]. Substituting K or P by other cations (Rb, As, ...) leads to isomorphous compounds exhibiting the same phase transition. A special case is the substitution of K by an ammonium group : the resulting species

$NH_4H_2PO_4$ (ADP), $NH_4H_2AsO_4$ and their deuterated equivalents are paraelectric and isomorphous to KDP at room temperature, but undergo upon cooling a transition to an antiferroelectric (AFE) phase, firstly identified by Nagamiya [3]. This originates from the peculiar topology of the ammonium sites, the protons of which point towards neighbor oxygens leading to a local AFE arrangement of acid protons [4]. The studies of this AFE phase are difficult because the samples shatter upon cooling below T_N. The only results about the dynamic properties of the AFE phase were published very recently : low-frequency infrared reflectivity spectra [5, 6], and Raman scattering spectra [7]. Infrared reflectivity spectroscopy is particularly interesting because it provides the lattice mode contribution to the dielectric constant, the direct accurate measurement of which by classical dielectric techniques is not reliable on shattered samples. The lattice mode contribution to the dielectric constant in the PE phase was already measured by submillimetric dielectric spectroscopy, from room temperature down to $T_N + 1$ K [8]. But even in the PE phase, the temperature dependence of the infrared spectra in a wide frequency range, including the internal modes of PO_4^{3-} tetrahedra has not yet been reported to our knowledge. The aim of the present paper is to report the infrared reflectivity spectra of ADP in the PE and AFE phases, in a larger frequency range than references [5, 6]. The factorized form of the dielectric constant is fitted to the experimental spectra, in order to provide the structure of the polar modes. The results are discussed in the light of a preceding work on the FE KDP-type compounds [9], in order to identify the vibration modes and to compare the FE and AFE tendencies. Another interest for the present work following reference [9] is to deal with the poles of the phase diagram of the system $Rb_{1-x}(NH_4)_xH_2PO_4$ (RADP), the middle of which exhibiting structural glass properties at low temperatures (for a review, see [10]).

2. Experimental procedure.

The infrared reflectivity spectra were obtained with a Bruker IFS 113C rapid-scan Fourier-transform interferometer, giving access to the spectral range 20-4 000 cm^{-1}. The samples are cut into thin plates ($10 \times 10 \times 1$ mm^3), with the fourfold axis lying in the face, and carefully sealed with silver paint on the cryostat sample holder. Good sticking of the sample is necessary to keep correct optical quality at the surface of the shattered sample, upon cooling below the phase transition. The low-temperature device is a temperature-controlled liquid nitrogen cryostat, the temperature stability of which is better than 0.1 K.

3. Symmetry of the vibration modes.

At room temperature, ADP belongs to the tetragonal class, with space group $I\bar{4}2d$, and two formulas per primitive unit cell. The averaged position of the proton is in the middle of the O—H—O bonds, perpendicularly to the fourfold c-axis. Below $T_N = 148$ K, the O—H—O bonds become asymmetric, with two protons localized on each PO_4 tetrahedron. Contrary to the case of its FE isomorphs, where two « upper » or two « lower » (with respect to the c-axis) proton sites are filled for an arbitrary H_2PO_4 group, ADP has one « upper » and one « lower » site filled in its AFE phase. The low-temperature space group is $P2_12_12_1$, with four formulas per unit cell. The AFE axis can be either a- or b-axis, the multi-domain structure which follows induces the sample shattering at the phase transition [11].

Tables I (already reported in [4]) and II give the decomposition of the zone-center lattices modes into irreducible representations, in the high- and low-temperature phases. The infrared spectra for orientation of the electric field of the IR electromagnetic wave along (resp. perpendicular to) the z-axis correspond to B_2 (resp. E) symmetry above T_N, and

Table I. — *Reduction into irreducible representations of the* 72 *zone-center modes of* ADP *in the paraelectric phase* ($I\bar{4}2d$ *space group). g denotes the degeneracy of the representation,* N_{tot} *the total number of modes,* N_{Ac}, N_T *and* N_H *the number of acoustical, translational external, and proton modes, respectively.* N_L *and* N_{int} *are the number of libration and internal modes for both tetrahedra species,* PO_4 *and* NH_4. *The internal modes are detailed with Herzberg's notations.*

	g	N_{TOT}	N_{Ac}	N_T	$N_L(PO_4)$	$N_L(NH_4)$	N_H	$N_{int}(PO_4)$	$N_{int}(NH_4)$	Basis functions. Raman and IR activities
A_1	1	7	0	0	1	1	1	$1\nu_1 + 1\nu_2$	$1\nu_1 + 1\nu_2$	$xx + yy$, zz
A_2	1	8	0	0	1	1	2	$1\nu_1 + 1\nu_2$	$1\nu_1 + 1\nu_2$	—
B_1	1	9	0	2	0	0	1	$1\nu_2 + 1\nu_3 + 1\nu_4$	$1\nu_2 + 1\nu_3 + 1\nu_4$	$xx - yy$
B_2	1	10	1	1	0	0	2	$1\nu_2 + 1\nu_3 + 1\nu_4$	$1\nu_2 + 1\nu_3 + 1\nu_4$	xy, P_z
E	2	19	1	3	2	2	3	$2\nu_3 + 2\nu_4$	$2\nu_3 + 2\nu_4$	yz, P_x xz, P_y

Table II. — *Reduction into irreducible representations of the* 144 *zone-center modes of* ADP *in the* AFE *phase* ($P2_12_12_1$ *space group). For notations, see table* I.

	g	N_{TOT}	N_{Ac}	N_T	$N_L(PO_4)$	$N_L(NH_4)$	N_H	$N_{int}(PO_4)$	$N_{int}(NH_4)$	Basis functions. Raman and IR activities
A	1	36	0	6	3	3	6	$1\nu_1 + 2\nu_2 + 3\nu_3 + 3\nu_4$	$1\nu_1 + 2\nu_2 + 3\nu_3 + 3\nu_4$	xx, yy, zz
B_1	1	36	1	5	3	3	6	$1\nu_1 + 2\nu_2 + 3\nu_3 + 3\nu_4$	$1\nu_1 + 2\nu_2 + 3\nu_3 + 3\nu_4$	xy, P_z
B_2	1	36	1	5	3	3	6	$1\nu_1 + 2\nu_2 + 3\nu_3 + 3\nu_4$	$1\nu_1 + 2\nu_2 + 3\nu_3 + 3\nu_4$	xz, P_y
B_3	1	36	1	5	3	3	6	$1\nu_1 + 2\nu_2 + 3\nu_3 + 3\nu_4$	$1\nu_1 + 2\nu_2 + 3\nu_3 + 3\nu_4$	yz, P_x

B_1 (resp. $B_2 + B_3$) below T_N. The polydomain structure below T_N prevents to obtain the B_2 and B_3 spectra separetely.

The symmetry elements lost at the phase transition correspond to the condensation of a symmetry-breaking mode at the Z-point (001) of the high-temperature Brillouin zone. Table III gives the decomposition into irreducible representations of the Z-point vibration modes expressed in Zak's notations [12], and the correlation between (i) modes at points Γ and Z of the paraelectric phase and (ii) modes at the Γ-point of the AFE phase. Note that at the Z-point, the three irreducible representations are doubly degenerated. The high-temperature symmetry-breaking mode belongs to the representation ($Z_3 \oplus Z_5$), since it transforms below T_N according to the totally symmetrical representation A. Thus, an eventual

Table III. — *Reduction into irreducible representations (expressed within Zak's notations* [12]) *of vibration modes of* ADP *in the paraelectric phase at the Z-point of the Brillouin zone, and correlation between* (i) *high-temperature Z- and Γ-modes, and* (ii) *low temperature Γ-modes. The doubly degenerated representations are indicated in parenthesis.*

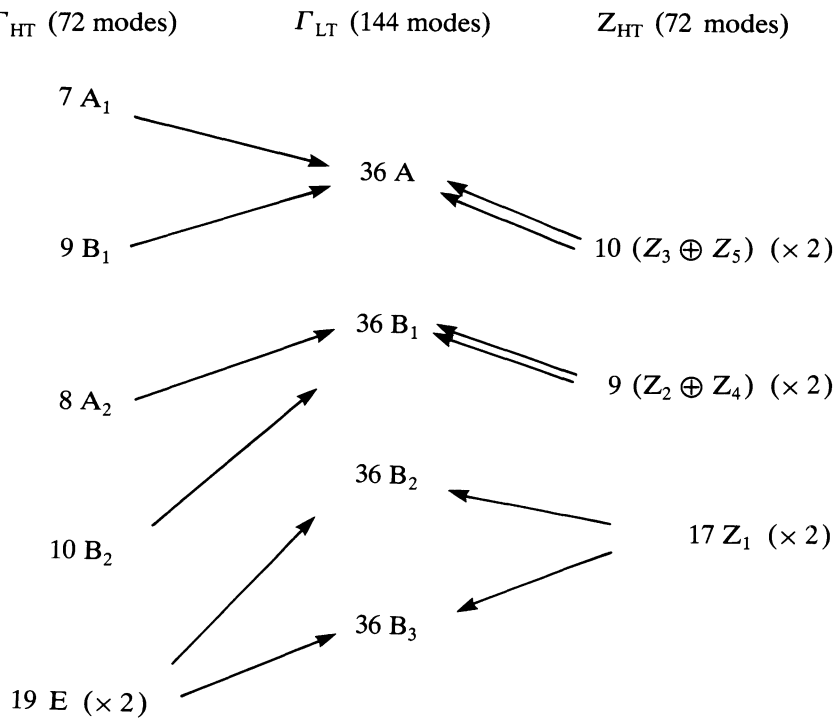

high-temperature soft-mode would be doubly degenerate (corresponding to the two possible orientations of the AFE axis below T_N), and it would split below T_N in two components, each of them belonging to the totally symmetrical representation A. Both components would then be infrared inactive (Tab. II). No experimental evidence for these AFE modes has been reported up to now, but a temperature-dependent quasi-elastic component was observed by neutron scattering in the PE phase just above T_N in deuterated ADP at the Z-point [13], which was interpreted as a condensing highly-damped mode.

4. Analysis of infrared reflectivity spectra.

The procedure to extract lattice mode parameters from the experimental spectra consists in fitting a model of dielectric function to the experimental spectra. The most convenient of these models is the factorized form of the dielectric function, or generalized Kurosawa relation :

$$\varepsilon(\omega) = \varepsilon_\infty \prod_j \frac{(\Omega_{jLO}^2 - \omega^2 + i\omega\gamma_{jLO})}{(\Omega_{jTO}^2 - \omega^2 + i\omega\gamma_{jTO})} \tag{1}$$

where Ω_{jTO} and Ω_{jLO} are the transverse and longitudinal frequencies of mode j, and γ_{jTO} and γ_{jLO} the corresponding dampings. This model has been already successfully applied to many cases [14].

The oscillator strength of the j-th mode can be calculated from the whole set of TO and LO frequencies :

$$\Delta\varepsilon_j = \varepsilon_\infty \, \Omega_{j\mathrm{TO}}^{-2} \frac{\prod_k (\Omega_{k\mathrm{LO}}^2 - \Omega_{j\mathrm{TO}}^2)}{\prod_{k \neq j} (\Omega_{k\mathrm{TO}}^2 - \Omega_{j\mathrm{TO}}^2)} \tag{2}$$

and the static dielectric constant is given by

$$\varepsilon(\omega = 0) = \varepsilon_\infty + \sum_j \Delta\varepsilon_j \tag{3}$$

5. Results and discussion.

The experimental spectra (Fig. 1) were obtained from liquid nitrogen up to room temperature. As previously shown by Wyncke *et al.* [5] for low frequencies, the shattering of the samples at T_N does not alter the quality of the infrared reflectivity spectra in the AFE phase, apart from a reduction of the signal-to-noise ratio at high frequencies (above 1 500 cm^{-1}), due to diffusion at the surface. No depolarization effect is visible in the experimental spectra at 78 K (Fig. 1) : each spectrum presents some reflection bands which are not observed in the spectrum obtained with the electric field of the infrared wave rotated by 90°. Moreover, the spectra in the PE phase taken before and after cooling below T_N are identical within experimental error.

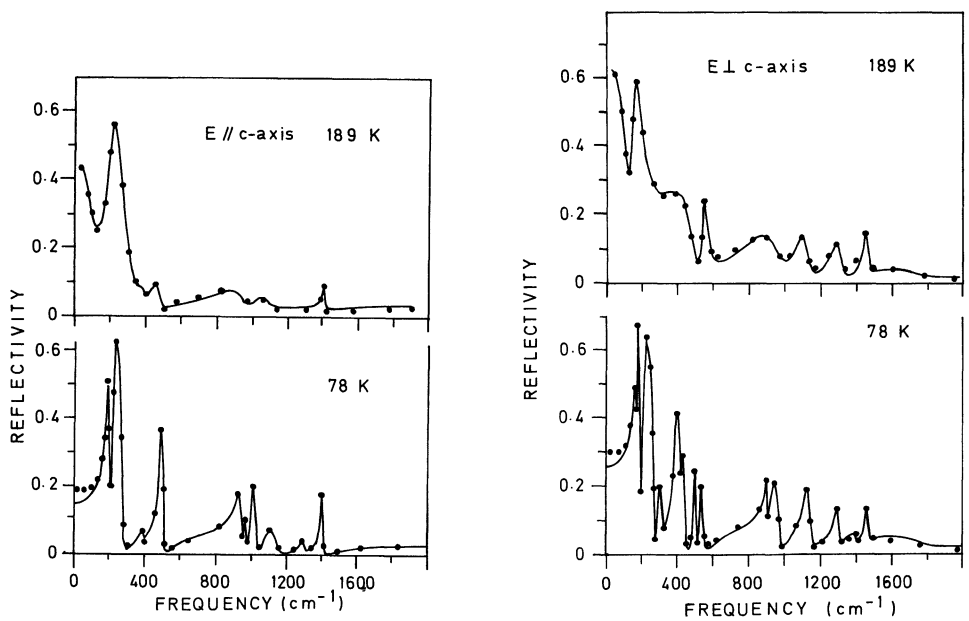

Fig. 1. — Typical infrared reflectivity spectra of ADP in the para- and antiferroelectric phases, with electric field of the IR electromagnetic wave polarized along (a) or perpendicular to (b) the c-axis. Full circles : experimental spectra ; full lines : best fits performed with the factorized form of the dielectric function (Eq. (1)).

All spectra were simulated with model equation (1). From the resulting set of frequencies and dampings, one obtains the TO-mode structure (Fig. 2), which is given by the imaginary part of the dielectric function. In the PE phase, the spectra are practically temperature independent, apart from the lowest-frequency mode in both polarizations. The spectra are simulated in the PE phase with 7 modes for polarization along the *c*-axis and 10 modes perpendicular to it, while 9 and 18 optic modes (Tab. I) are symmetry allowed, respectively. This discrepancy originates from (i) modes of too high frequency ($\nu_3\,NH_4$), (ii) too weakly polar modes (librations) and (iii) a group of modes insufficiently splitted (translation modes in the E spectrum). The mode assignment is given in figure 2. Apart from the sharp supplementary NH_4 modes, in the PE phase, the spectra are very similar to those of KDP and RDP, with phonon lines broadened by the proton response. This proton response is even so broad that some phonon profiles are characteristic of Fano interferences between a continuum and a discrete state, particularly in the 400-500 cm^{-1} spectral range. The TO-mode structure is practically constant in the whole PE phase. Note that as in KDP [9], the lowest-frequency highly-damped mode, which is the strongest polar one, is symmetry-forbidden in the space group $I\bar{4}2d$. This space group stands for the averaged position of protons, between their two sites, and then the supplementary degree of freedom corresponding to the intersite

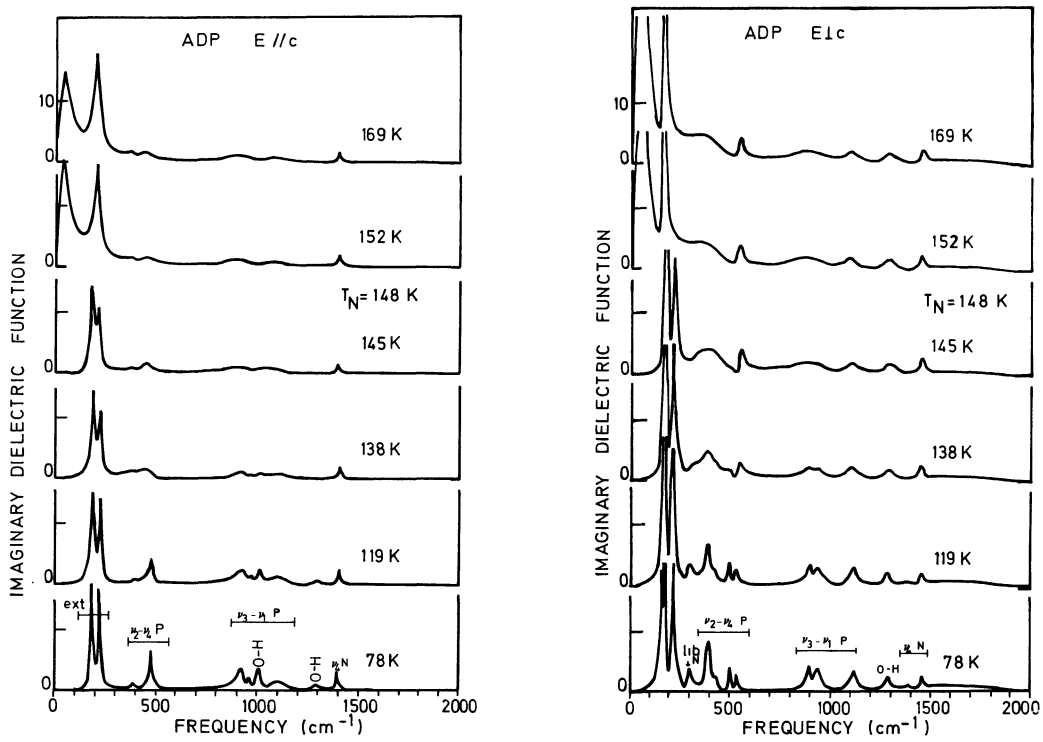

Fig. 2. — Temperature dependence of the structure of TO modes (imaginary part of the dielectric function) of ADP, obtained by fitting equation (1) to the experimental spectra, for IR electric field parallel (a) and perpendicular (b) to *c*-axis. The TO-mode structure at other temperatures in the PE phase are very similar to the 169 K data and are not plotted here for sake of simplicity. The mode assignment is indicated on the 78 K spectra ; P and N denote modes of the PO_4 and NO_4 tetrahedra, respectively.

proton motions is not taken into account in the number of modes given in table I. The low-frequency extra mode is due to this supplementary degree of freedom. But an important difference with KDP is that in the present case, this highly-damped mode is observed in both spectra (B_2 and E), while it is visible only in B_2 symmetry in the PE phase of FE compounds. Figure 3 displays the temperature dependence of TO- and LO-mode frequencies in the far infrared, obtained by the fitting. The essential feature concerns the lowest-frequency mode in both polarizations, which slightly softens upon cooling down to T_N, and suddenly disappears just below the phase transion. Apart from the splittings and the appearance of new allowed modes due to the symmetry lowering at T_N, the other modes do not present noticeable changes in temperature.

5.1 LATTICE MODES IN THE AFE PHASE. — In the AFE phase, 36 modes are symmetry-allowed for B_1 spectra and 72 for the other orientation $B_2 + B_3$. The number of modes used for fitting of the 78 K spectra is much smaller (10 for B_1, 17 for $B_2 + B_3$), due to (i) the same reasons as in the PE phase from one part, but also to (ii) a too small dispersion of modes when compared to the linewidths, after the Brillouin-zone folding. The comparison of the low-temperature (≈ 80 K) phonon spectra of AFE ADP with those of FE RDP is of interest (Fig. 4). At this temperature, the phonon linewidths and the effects directly connected to the phase transition are minimized and one can consider the differences between the dynamics of the two structures. The lattice modes will be discussed by increasing order of frequency.

5.1.1 *Translation and libration modes.* — Of course, the translation external modes lie at lower frequencies in RDP than in ADP, due to the difference of the cation masses. In the

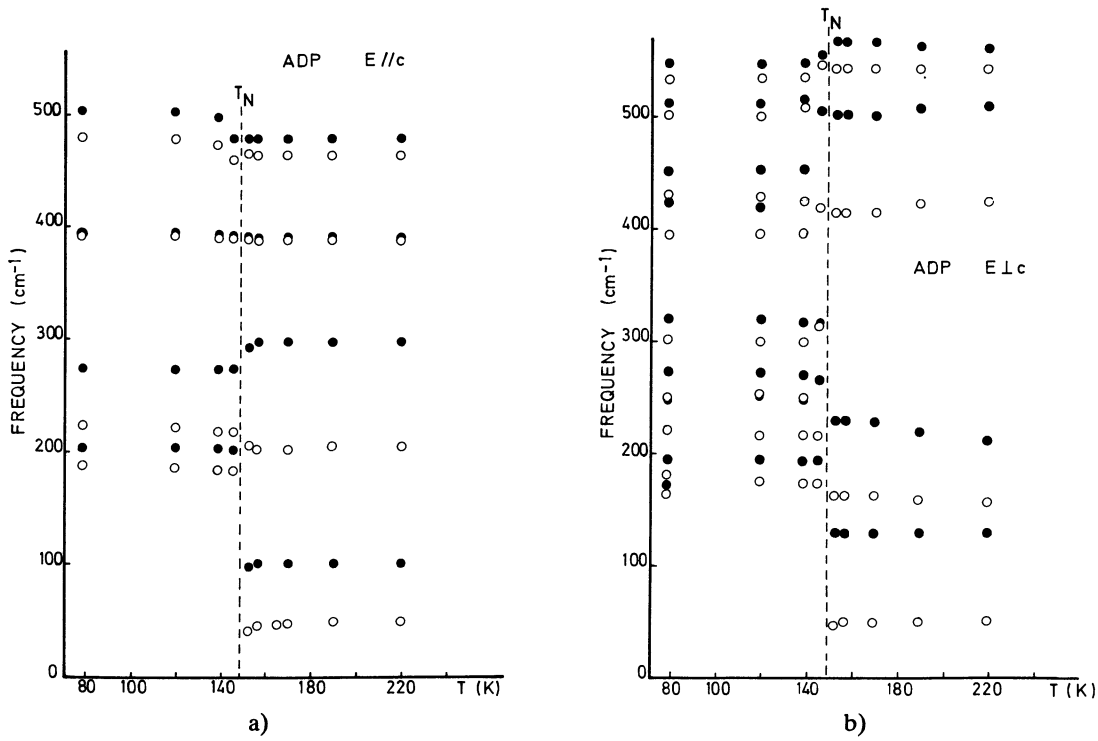

Fig. 3. — Temperature dependence of TO (open circles) and LO (full circles) mode frequencies, for IR electric field parallel (a) and perpendicular (b) to *c*-axis.

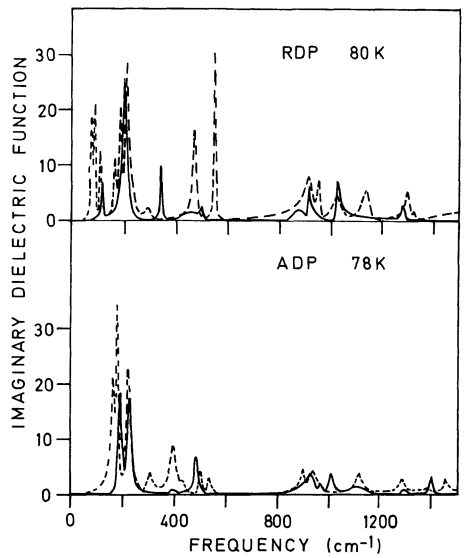

Fig. 4. — Lower part : TO-mode structure of ADP at 78 K, for B_1 (full line) and $B_2 + B_3$ (dashed line) symmetries. Upper part : TO-mode structure of RDP at 80 K [9], for corresponding orientations, i.e., A_1 (full line) and $B_1 + B_2$ (dashed line), plotted here for comparison.

$B_2 + B_3$ spectrum, the small mode at 302 cm^{-1} is attributed to NH_4 librations, since these motions were unambiguously observed at 306 cm^{-1} in Raman spectra [4], which are more sensitive than infrared spectroscopy to these weakly polar motions. This NH_4 libration is observed only in one polarization (electric field in the AFE axis plane). The weak mode previously reported in this spectral range in the infrared spectra of RDP, but not of KDP [9], lies at lower frequency (293.5 cm^{-1}) and is not observed by Raman scattering [15], it is then assigned to a translation mode (infrared active but only weakly Raman active, contrary to libration modes).

5.1.2 *ν_2 and ν_4 PO_4 internal modes.* — Of high interest is the behavior of the PO_4 internal modes. In the 400-500 cm^{-1} spectral range, for polarization along the *c*-axis, the ν_{4c} internal mode has a completely different behavior in the two compounds : this mode is strongly damped in RDP, with a damping-over-frequency ratio equal to 17 % (30 % in KDP), whereas in ADP this ratio is about 3 %. These high damping values in ferroelectric crystals are due to a multicomponent interaction with the collective tunneling proton mode and with the translational external mode, the result of which is the FE soft mode itself [9]. In compounds where this three-components interaction does not occur, mode ν_{4c} has no reason to be heavily damped. Effectively, in KD_2PO_4 [16], where tunneling does not play a significant role, or in the present case of ADP where the collective proton mode has not the same eigenvector pattern and then does not couple with mode ν_{4c}, one observes smaller damping-over-frequency ratios.

The weak mode lying at 394 cm^{-1} at 78 K in the B_1 spectrum and observed in both phases is ascribed to a PO_4 ν_2 mode, corresponding to a Raman mode in the PE phase [4, 7]. There is a discrepancy *vs.* the results of Kasahara *et al.* [7] in the AFE phase who reported a splitting of this mode in two components (355 and 412 cm^{-1}) at 109 K. In the PO_4 ν_4 range, one polar mode is unambiguously observed in the infrared spectra (Fig. 2) while four components are

weakly Raman active, none of which corresponding to the infrared mode (TO or LO part). In the other polarization, in the *c*-plane, four TO modes lie in this spectral range at 78 K, at 396, 430.5, 501 and 533 cm^{-1}, the former one having the strongest oscillator strength ($\Delta\varepsilon$ = 0.63, 0.06, 0.1 and 0.07 respectively). Two ν_2 and three ν_4 are allowed by symmetry in this spectral range (which are each one allowed to split into two components by the lifting of degeneracy from E modes to B_2 and B_3 modes). The 396 cm^{-1} mode is essentially of ν_4 character, as indicated by its high oscillator strength. The fact that its frequency corresponds to ν_2 modes in other symmetries (Raman spectra [4, 7], and B_1 spectrum in the present paper) shows that in the *c*-plane, all modes interact in this spectral range and transfer their eigenvectors and oscillator strengths to their lower-frequency neighbor.

5.1.3 *Internal* PO_4 ν_1 *and* ν_3, *internal* NH_4, *and proton modes.* — In the near-infrared spectral range (800-2 000 cm^{-1}), the comparison of the three FE salts has enabled to identify the vibration modes [9]. The spectra of ADP exhibit supplementary modes, assigned to ν_4 internal vibrations of NH_4 tetrahedra, because of their frequencies (1 399.5, 1 395 and 1 456 cm^{-1}, very close to the fundamental frequency 1 397 cm^{-1}), and oscillator strengths which are too strong for an assignment to weakly polar ν_2 modes. The other NH_4 internal modes lie at higher frequencies (above 3 000 cm^{-1}), in a spectral range where the signal-to-noise ratio is too small to identify them unambiguously. The PO_4 ν_3 mode at 1 105 cm^{-1} is of interest : for the IR electric field oriented along the *c*-axis, it is not observed in the PE and FE structures, but only in the AFE structure. On the contrary, in the other polarization, the O—H mode at 1 035 cm^{-1} occurs only in the FE phase, whereas it is not observed in the AFE structure, nor in the PE one. Both modes constitute a good probe of local FE or AFE tendencies, which is particularly interesting for future investigations in RADP structural glasses.

5.2 PE-AFE PHASE TRANSITION. — As previously mentioned, the dominant feature at the phase transition is the occurrence in both orientations in the whole PE phase of strongly damped polarization fluctuation modes at low frequencies, which completely disappear just below T_N. The occurrence of these modes below T_N reported in a previous paper [17] was an artefact probably due to light scattering in the shattered structure. The other lattice modes are slightly broadened upon heating above T_N, due to the occurrence of intersite proton motions, but the highest-frequency ones, especially the NH_4 ν_4 modes, are practically unaffected by the phase transition. In the *c*-plane, where lies the AFE axis, the lowest-frequency mode is slightly overdamped, and slightly underdamped in the other polarization, along the *c*-axis. Figure 5 displays the temperature dependence of the oscillator strength of these two modes, obtained from the results of the simulation *via* equation (2), for both polarizations. The dielectric constant values, calculated by equation (3), are also plotted on the same diagram. In the AFE phase, the dielectric constant calculated from the spectra perpendicular to *c*-axis corresponds to an average value between the values ε_a and ε_b of the orthorhombic tensor ε, because of the polydomain structure. In the PE phase, it is obvious that the lowest-frequency mode oscillator strength explains 85 % to 90 % of the static dielectric constant in the two geometries. This large oscillator strength, increasing upon approaching T_N, combined with the frequency lowering, shows a tendency to softening of these modes. All this evidences a weak « improper ferroelectric » character for these low-frequency modes, which originates from the zone-corner instability by some coupling mechanism, more efficient in the *c*-plane (lower frequency, overdamped mode, higher oscillator strength) than along the *c*-axis, as predicted theoretically in pseudospin models [2, 18]. This is consistent with the orientation in the *c*-plane of the AFE axis, where the polarization fluctuations are expected to be maximum. The disappearance of these modes just below T_N, an anomalous feature upon undergoing a

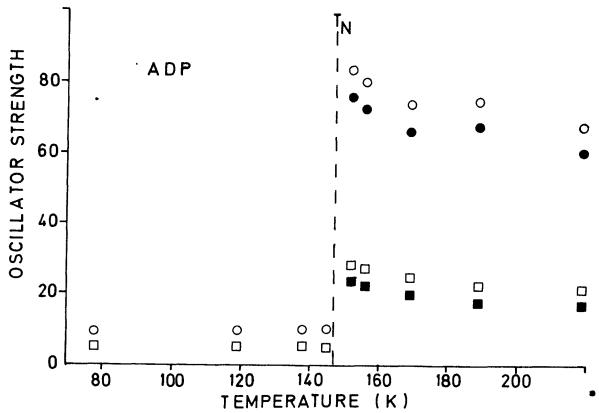

Fig. 5. — Temperature dependence of the oscillator strength of the highly-damped mode in the PE phase (full symbols), and dielectric constant (open symbols), deduced from simulation of the spectra with equation (1), in the two polarizations : electric field of the IR electromagnetic wave oriented along (squares) or perpendicular to (circles) the *c*-axis.

transition from a space group to a subgroup, correspond to the lack of one degree of freedom : the intersite motions of protons. Like in the B_2 spectrum of PE-FE compounds, the lowest-frequency modes originate from the proton motions. So, they do not appear in the modes allowed by symmetry in the space group $I\bar{4}2d$ (Tab. I), since this space group stands for the averaged position of protons. In FE compounds, the lowest-frequency mode, which is the ferroelectric soft mode, comes from the interaction between the proton motions and at least one lattice mode [9, 19]. This is evidenced by the noticeable temperature dependence of these lattice modes (frequency, damping and oscillator strength). On the contrary, there is no such temperature dependence for polar modes in ADP, apart from the lowest-frequency one. It is then highly probable that a mechanism analoguous to KDP occurs in ADP, but at the Brillouin zone boundary, which precludes to observe any effect in the infrared spectra : the proton motions would interact with a lattice mode at the *Z*-point of the Brillouin zone, resulting in the AFE instability. Thus, the AFE instability couples with the zone-center lowest-frequency modes in each polarization, as evidenced by their frequency lowering upon approaching T_N.

A generally straightforward application of infrared reflectivity spectroscopy is the determination of the ionic effective charges, but this determination needs the knowledge of the *whole* set of TO and LO frequencies we do not have in the present case : the frequencies of the NH_4 ν_1 and ν_3 internal modes, and also of O—H stretching modes, are not known due to insufficient signal-to-noise ratio in this high-frequency spectral range, and the contribution of the high-frequency modes is essential in the effective charge calculation. Thus, contrary to the case of FE compounds [9], it is not possible for ADP to report the temperature dependence of the effective ionic charges, in order to evidence a possible pairing of cation-anion bonds at the phase transition.

6. Conclusion.

Summarizing, this study confirms that (i) a sample shattering does not preclude to perform infrared reflectivity spectroscopy in polarized light. About the dynamics of ADP, the essential conclusions can be given by comparison with the case of KDP-type ferroelectrics. (ii) The

spectra of KDP and ADP are very similar in the paraelectric phase, apart from the low-frequency range : a highly-damped mode of weak improper ferroelectric character occurs in both polarizations (B_2 and E) in ADP, whereas in KDP, no such mode is observed in the E spectrum while the B_2 one is dominated by the very strong ferroelectric soft mode. (iii) The most striking effect of the phase transition of ADP is the sudden disappearance of the lowest-frequency highly-damped modes just at T_N in both polarizations, while in the KDP or RDP ferroelectric phases, the overdamped mode is observed down to several ten degrees below T_c. This low-frequency component in ADP is coupled with the AFE instability, which itself originates from the coupling of intersite proton motions with lattice modes at the Brillouin zone boundary. (iv) Another important difference between ADP and KDP in ther low-frequency phases is the behavior of the ν_4 PO_4 internal mode, which confirms the role of this mode in the mechanism of ferroelectricity in KDP-type compounds.

Acknowledgements.

I am indebted to Pr. G. Hauret for providing the samples, and to Dr. A. Bulou for helpful discussions about group theory. Particular mention is made of Dr. F. Gervais for numerous and fruitful discussions.

References

[1] LINES M. E. and GLASS A. M., Principles and Applications of Ferroelectric and Related Materials (Clarendon, Oxford) 1977.
[2] BLINC R. and ZEKS B., Soft Modes in Ferroelectrics and Antiferroelectrics (North-Holland, Amsterdam) 1974.
[3] NAGAMIYA T., *Progr. Theor. Phys.* **7** (1952) 275.
[4] COURTENS E. and VOGT H., *J. Chim. Phys. Paris* **82** (1985) 317
[5] WYNCKE B., BREHAT F. and ARBOUZ H., *Phys. Stat. Sol. b* **134** (1986) 523.
[6] BREHAT F., WYNCKE B. and ARBOUZ H., *J. Phys. C* **19** (1986) 6893.
[7] KASAHARA M., TOKUNAGA M. and TATSUZAKI I., *J. Phys. Soc. Jpn.* **55** (1986) 367.
[8] VOLKOV A. A., KOZLOV G. V. and LEBEDEV S. P., *Fiz. Tverd. Tela* **22** (1980) 3064 (*Sov. Phys. Solid State* **22** (1980) 1789).
[9] SIMON P., GERVAIS F. and COURTENS E., *Phys. Rev. B* **37** (1988) 1969.
[10] COURTENS E., *Ferroelectrics* **72** (1987) 229.
[11] FUKAMI T., AKAHOSHI S., HUKUDA K. and YAGI T., *J. Phys. Soc. Jpn.* **56** (1987) 2223.
[12] ZAK J., CACHER A., GLÜCK M. and GUR Y., The Irreducible Representations of Space Groups (Benjamin, New York) 1969.
[13] MEISTER H., SKALYO Jr, J., FRAZER B. C. and SHIRANE G., *Phys. Rev.* **184** (1969) 550.
[14] GERVAIS F., Infrared and Millimeter Waves, Eds. K. J. Button (Academic Press, New York) **8** (1983) ch. 7, p. 279.
[15] PEERCY P. S. and SAMARA G. A., *Phys. Rev. B* **8** (1973) 2033.
[16] KAWAMURA T., MITSUISHI A., FURUYA N. and SHIMOMURA O., *Opt. Commun.* **10** (1974) 337.
[17] SIMON P. and GERVAIS F., *Ferroelectrics* **80** (1988) 209.
[18] BANERJEE S., NATH D. and CHAUDHURI B. K., *Phys. Rev. B* **24** (1981) 6469.
[19] KOBAYASHI K., *J. Phys. Soc. Jpn.* **24** (1968) 497.